ORIGINAL ARTICLE
Iran J Allergy Asthma Immunol
In press.

Multi-omics Profiling Reveals the Dynamics of Macrophage Polarization and T-cell Infiltration in Renal Fibrosis

Seyed Amirhossein Fazeli[1,2], Alireza Dadfar[3], Alireza Baghaeiaria[4], Samin Baktash[3], Elnaz Abbasi[4], and Amir-Reza Javanmard[2,5]

[1] Taleghani General Hospital, Division of Nephrology, Department of Internal Medicine, School of Medicine, Shahid Beheshti University of Medical Sciences, Tehran, Iran
[2] Iranian Dry Lab on Kidney Diseases (IDKD), School of Advanced Technologies in Medicine, Shahid Beheshti University of Medical Sciences, Tehran, Iran
[3] Department of Molecular Genetics, Faculty of Biological Sciences, Tarbiat Modares University, Tehran, Iran
[4] Tehran Medical Sciences Branch, Islamic Azad University, Tehran, Iran
[5] Clinical Research and Development Center, Shahid Modarres Hospital, Shahid Beheshti University of Medical Sciences, Tehran, Iran

Received: 21 May 2026; Received in revised form: 2 July 2026; Accepted: 19 July 2026

IN PRESS

ABSTRACT

Renal fibrosis is a progressive, immune-mediated pathology driven by chronic inflammation and abnormal tissue repair. Although macrophages and T-cells are critical mediators of immune responses, their spatiotemporal dynamics and specific crosstalk within the fibrotic microenvironment remain poorly defined. This study utilized an integrative bioinformatics approach to characterize the immunological landscape of kidney fibrosis.

Publicly available bulk transcriptomic, proteomic, single-cell RNA sequencing (scRNA-seq), and spatial transcriptomics datasets from fibrotic and healthy kidneys were systematically analyzed. Standardized bioinformatics pipelines were employed for dimensional reduction, differential expression, and pathway enrichment. Pseudotime trajectory inference (Monocle3) and cell-cell communication analysis (CellChat) were utilized to map immune cell transitions and receptor-ligand interactions.

Integrative bulk multi-omics analysis identified a distinct immune-fibrotic molecular signature highly correlated with disease severity. High-resolution scRNA-seq revealed a temporal phenotypic shift in macrophages, transitioning from an early pro-inflammatory state to a late pro-fibrotic state characterized by Spp1 and Mrc1 expression. Concurrently, T cell profiling demonstrated a significant immunological imbalance, marked by enhanced infiltration of Th17 cells (IL 17A+ CD4+) and a depletion of regulatory T-cells (Foxp3+). Cell-cell communication networks highlighted the CXCL16-CXCR6 axis as a key driver of T-cell recruitment, alongside robust TGF-β signaling mediating macrophage-T cell-fibroblast crosstalk. Furthermore, spatial transcriptomics validated the physical co-localization of pro-fibrotic macrophages and Th17 cells within active fibrotic niches.

Corresponding Author: Amir-Reza Javanmard, PhD; Iranian Dry Lab on Kidney Diseases (IDKD), School of Advanced Technologies in Medicine, Shahid Beheshti University of Medical Sciences, Tehran, Iran. Tel: (+98 21) 230 311, Fax: (+98 21) 230 311, Email: j.amirreza@modares.ac.ir

Copyright©, Iran J Allergy Asthma Immunol. All rights reserved.

Published by Tehran University of Medical Sciences (http://ijaai.tums.ac.ir)

This integrative multi-omics analysis maps the dynamic interplay between macrophage polarization and T cell infiltration during renal fibrogenesis. The identified immunological networks, particularly the spatial and temporal coupling of pro-fibrotic macrophages and Th17 cells, offer novel insights into the immune pathogenesis of kidney fibrosis and highlight potential targeted immunotherapeutic strategies.

Keywords: Macrophage polarization; Renal fibrosis; Single-cell RNA sequencing; Spatial transcriptomics; Th17 Cells; Tumor necrosis factor-alpha

INTRODUCTION

Chronic kidney disease (CKD) is a global health burden, progressing inevitably to end-stage renal disease (ESRD) regardless of the primary etiology.[1] The common pathological hallmark of progressive CKD is renal fibrosis, characterized by the excessive extracellular matrix (ECM) deposition, tubular atrophy, and microvascular rarefaction.[2] Recent immunological studies have established that renal fibrosis is not merely structural deterioration but a profoundly immune-mediated process. Following acute or chronic injury, the kidney microenvironment becomes infiltrated by various innate and adaptive immune cells that orchestrate the inflammatory and subsequent fibrotic cascades.[3,4]

Macrophages and T-cells are recognized as the primary immunologic drivers of renal fibrogenesis. Macrophages exhibit immense plasticity, conventionally categorized into early pro-inflammatory (M1-like) phenotypes that exacerbate tissue injury, and later anti-inflammatory, pro-fibrotic (M2-like) phenotypes that promote myofibroblast activation through the secretion of transforming growth factor-beta (TGF-β).[5,6] Concurrently, the adaptive immune response, particularly the imbalance between pro-inflammatory CD4+ Th17 cells and immunosuppressive Foxp3+ regulatory T cells (Tregs), dictates the severity of the fibrotic response.[7] However, the exact temporal dynamics of macrophage polarization, their spatial relationship with specific T cell subsets, and the intricate receptor-ligand crosstalk within the fibrotic niche remain incompletely understood.

Traditional bulk transcriptomic approaches lack the resolution to decipher the heterogeneity of these immune populations. The advent of single-cell RNA sequencing (scRNA-seq) and spatial transcriptomics provides an unprecedented opportunity to map the immune microenvironment at single-cell resolution while preserving spatial context.[8] In this study, we used a comprehensive bioinformatics approach, integrating publicly available bulk transcriptomics, proteomics, scRNA-seq, and spatial transcriptomics data from murine unilateral ureteral obstruction (UUO) models. Our objective was to delineate the temporal dynamics of macrophage polarization, characterize Tcell infiltration patterns, and map the critical intercellular communication networks driving immune-mediated renal fibrosis.

MATERIALS AND METHODS

Public Dataset Acquisition and Study Design

To investigate the immunological mechanisms of renal fibrosis, publicly available bulk transcriptomic, single-cell RNA sequencing (scRNA-seq), spatial transcriptomics, and proteomic datasets were retrieved from the Gene Expression Omnibus (GEO) and the Proteomics Identifications Database (PRIDE). Datasets derived from the Unilateral Ureteral Obstruction (UUO) murine model of kidney fibrosis (days 3, 7, and 14 post-UUO) and sham-operated controls were selected. Inclusion criteria required high-quality raw data formats (FASTQ or raw count matrices for RNA-seq, and RAW files for proteomics) and a minimum of three biological replicates per condition.

Bulk Transcriptomics and Proteomics Processing

Raw RNA-seq count matrices were imported into R (version 4.3.0). Differential expression analysis was performed using the DESeq2 package. Genes with an adjusted p-value (padj<0.05) and an absolute $\log_2$-fold change ($|\log_2 (FC)| \geq 1.0$) were defined as Differentially Expressed Genes (DEGs). For proteomics data, normalized intensity matrices were analyzed using the limma package. Differentially Expressed Proteins (DEPs) were identified using an empirical Bayes method, with significance thresholds set at padj<0.05 and $|\log_2 (FC)| \geq 1.0$. Gene Ontology (GO) and Kyoto Encyclopedia of Genes and Genomes (KEGG) pathway

IN PRESS

enrichment analyses were conducted using the clusterProfiler package.

Single-Cell RNA Sequencing (scRNA-seq) Quality Control and Integration

Raw scRNA-seq feature-barcode matrices were processed using the Seurat R package. Quality control (QC) was applied to remove low-quality cells and doublets. Cells expressing fewer than 200 or more than 2500unique genes, and those with a mitochondrial gene proportion of greater than10% (mt.percent>10%), were excluded from downstream analysis. Data were normalized using the LogNormalize method. Highly variable features were identified, followed by principal component analysis (PCA). Uniform Manifold Approximation and Projection (UMAP) was used for dimensionality reduction based on the first 20 principal components ($1 \leq PC \leq 20$). Graph-based clustering was performed using the FindClusters function at a resolution of 0.5. Cell types were annotated based on the expression of canonical marker genes.

Pseudotime Trajectory Inference

To evaluate the dynamic transition of macrophage polarization, pseudotime trajectory analysis was performed using the Monocle3 package. The subset of cells annotated as macrophages (M1-like and M2-like) was extracted from the Seurat object and converted into a cell_data_set object. Cells were ordered along a reconstructed trajectory based on gene expression changes, with the root node manually assigned to the early inflammatory macrophage cluster corresponding to day 3 post-UUO.

Cell-cell Communication Analysis

To infer intercellular communication networks, particularly between macrophages, T cells, and fibroblasts, the CellChat R package was used. The normalized scRNA-seq count matrix and cell annotations were used as input. The CellChatDB.mouse database was utilized as the reference for ligand-receptor interactions. Communication probabilities were calculated using a mass action model, and significant interactions were identified using a permutation test ($p<0.05$). Signaling pathways were visualized using chord diagrams and circle plots.

Spatial Transcriptomics Analysis

Publicly available Visium spatial transcriptomics data from fibrotic murine kidneys were analyzed using Seurat. Data were normalized using the SCTransform function to account for spatial variance. Dimensionality reduction and spatial clustering were performed. To integrate scRNA-seq data with spatial maps, expression signatures of specific subsets (e.g., Spp1+ macrophages and Il17a+ T cells) were mapped onto the spatial tissue coordinates using the SpatialFeaturePlot function to assess niche co-localization within fibrotic regions.

Statistical Analysis

All computational analyses and statistical tests were performed in R (version 4.3.0). The Wilcoxon rank-sum test was used for differential expression analysis of scRNA-seq data. Spearman correlation was used to assess the relationship between gene expression modules and fibrosis severity scores. Statistical significance was defined as $p<0.05$ unless otherwise specified by the specific bioinformatics tool's default parameters. To mitigate batch effects and technical variation across scRNA-seq datasets, data integration was performed using the Seurat integration method, ensuring that cells clustered by biological cell type rather than by batch origin.

RESULTS

Integrative Analysis of Public Bulk Transcriptomic and Proteomic Datasets Identifies a Core Immune-fibrotic Signature

To identify the core molecular drivers of renal fibrosis, we retrieved and integrated bulk transcriptomic (RNA-seq) and proteomic data from the murine UUO model (days 7 and 14) and sham controls. Differential expression analysis utilizing DESeq2 identified 1,245 differentially expressed genes (DEGs) ($padj<0.05$, $|\log_2(FC)| \geq 1.0$) (Figure 1A), while limma analysis of the proteomic datasets revealed 432 differentially expressed proteins (DEPs) (Figure 1B). Cross-referencing these datasets yielded an overlap of 215 genes/proteins consistently upregulated in fibrotic kidneys (Figure 1C, Table 1). Gene Ontology (GO) and KEGG pathway enrichment analyses of these shared targets demonstrated substantial enrichment in immune system activation pathways, specifically "cytokine-cytokine receptor interaction" ($p<0.001$) and "macrophage activation" ($p<0.01$), alongside classic extracellular matrix (ECM) organization pathways (Figure 1D).

IN PRESS

Table 1. Core overlapping immune-fibrotic targets.

Gene Symbol	Protein Name	Avg log2 (FC) log_2 (FC) log2 (FC) (Transcript)	Avg log2 (FC) log_2 (FC) log2 (FC) (Protein)	Adjusted *p*
Spp1	Osteopontin	4.85	3.92	1.2×10−14
Fn1	Fibronectin	4.12	3.45	4.5×10−12
Cxcl16	C-X-C motif chemokine 16	3.98	3.10	8.8×10−11
Tgfb1	Transforming growth factor beta-1	3.55	2.88	2.1×10−09
Il1b	Interleukin-1 beta	3.20	2.54	5.6×10−08
Mrc1	Macrophage mannose receptor 1	2.95	2.41	1.1×10−07
Tnf	Tumor necrosis factor	2.80	2.15	3.4×10−06

List of representative significantly upregulated targets identified in both bulk transcriptomic and proteomic analyses (padj<0.05), sorted by average log2 (FC).

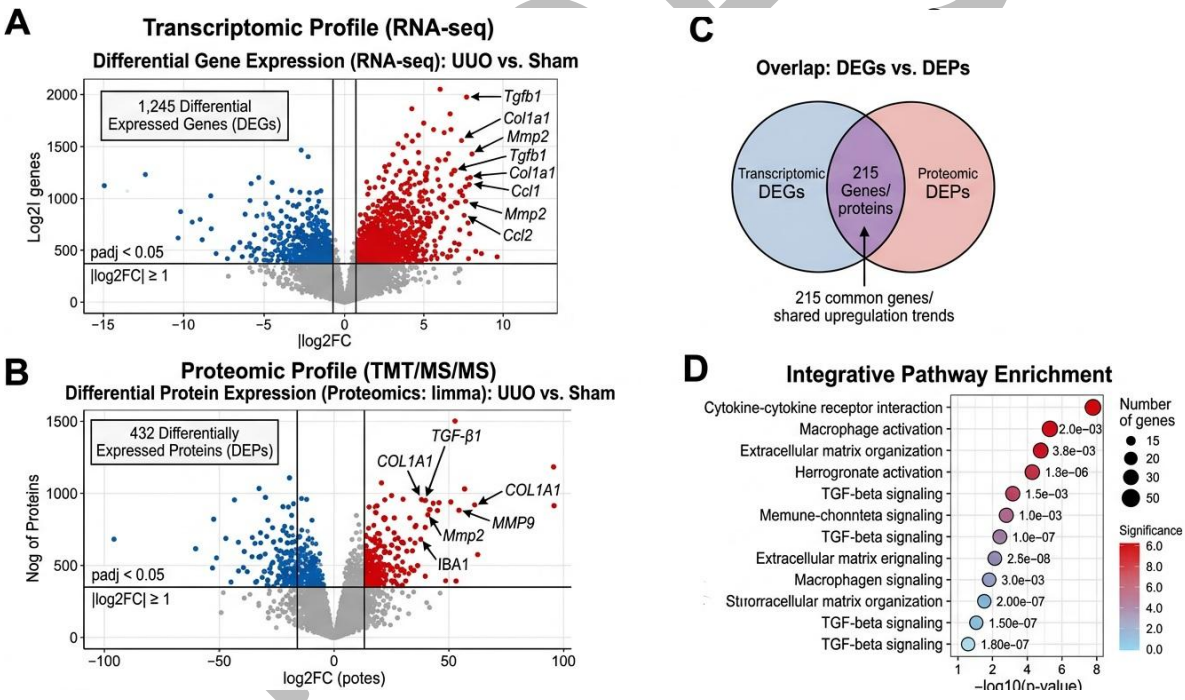

Figure 1. Integrative bulk transcriptomic and proteomic analysis reveals a core immune-fibrotic signature in murine renal fibrosis. (A) Volcano plot illustrating differentially expressed genes (DEGs) from public bulk RNA-seq data of Unilateral Ureteral Obstruction (UUO) versus sham kidneys. Significant DEGs (padj<0.05 and |log2 (FC)|≥1.0) are highlighted in red (upregulated) and blue (downregulated). (B) Volcano plot showing differentially expressed proteins (DEPs) identified via limma analysis of corresponding public proteomic datasets. (C) Venn diagram demonstrating the intersection of upregulated DEGs and DEPs, identifying 215 shared targets. (D) Bubble plot showing Gene Ontology (GO) and KEGG pathway enrichment analysis of the 215 shared targets, highlighting significant enrichment in "cytokine-cytokine receptor interaction" and "macrophage activation" pathways. The size of the bubbles represents the number of mapped genes, and the color gradient indicates the adjusted p-value.

Single-cell RNA Sequencing Reveals a Temporal Trajectory of Macrophage Polarization

To dissect the cellular heterogeneity driving the bulk tissue signatures, we analyzed public scRNA-seq datasets of UUO kidneys (days 3, 7, and 14). Following rigorous quality control, UMAP clustering successfully partitioned the myeloid compartment (Figure 2A). We observed a distinct temporal shift in macrophage subsets. At day 3 post-UUO, the predominant population exhibited a pro-inflammatory "M1-like" signature, characterized by high expression of Tnf, Il1b, and Cxcl10 (Figure 2B). By days 7 and 14, this population was largely replaced by a pro-fibrotic "M2-like" macrophage subset expressing high levels of Mrc1 (CD206), Arg1, and Spp1 (Osteopontin) (Figure 2C). Pseudotime trajectory inference using Monocle3 confirmed a continuous phenotypic transition from the early Il1b+ inflammatory state to the late Spp1+ pro-fibrotic state as disease progressed (Figure 2D).

scRNA-seq Uncovers Th17 Expansion and Treg Depletion in the Fibrotic Microenvironment

Sub-clustering of the lymphoid compartment revealed profound alterations in T-cell dynamics during fibrosis progression (Figure 3A). While the overall proportion of CD4+ T-cells increased in UUO kidneys compared to sham controls, the subtype composition shifted dramatically. We identified a significant expansion of a Th17-like cluster characterized by robust expression of Il17a, Rorc, and Il22, peaking at day 14 ($p<0.01$) (Figure 3B). Conversely, the proportion of regulatory T-cells (Tregs), marked by Foxp3 and Il10 expression, underwent a relative reduction over the same timeframe (Figure 3C, Table 2).

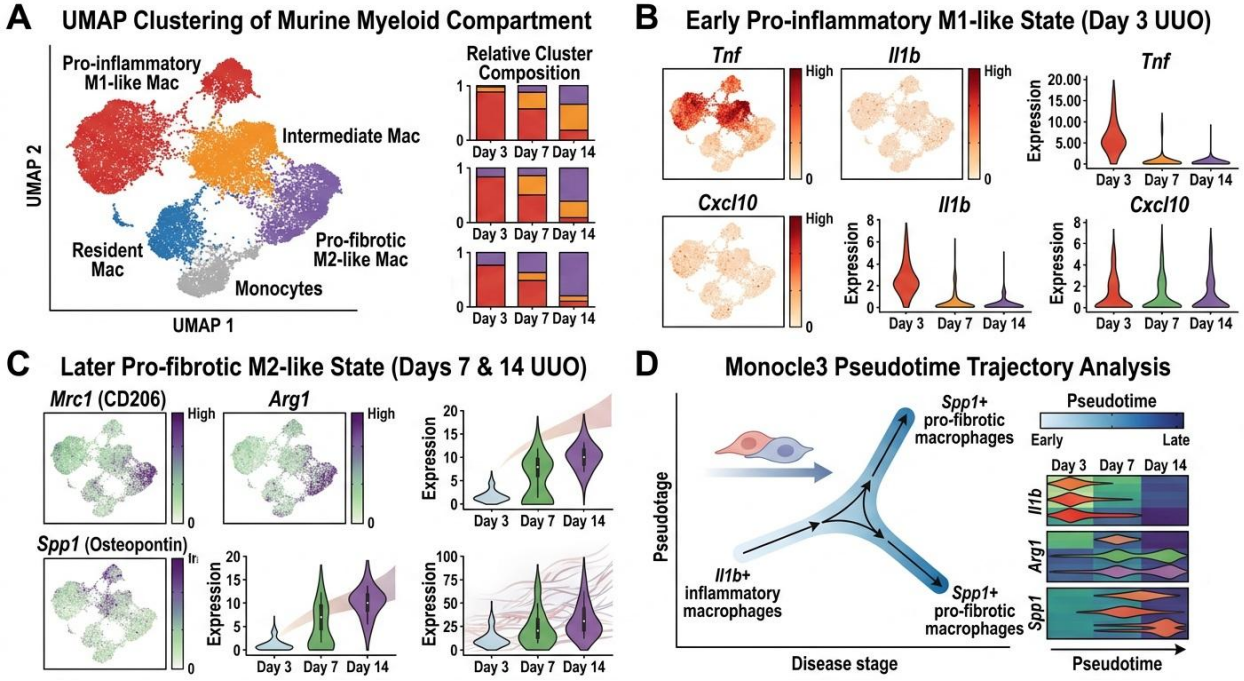

Figure 2. Single-cell RNA sequencing analysis maps the temporal trajectory of macrophage polarization.
(A) Uniform Manifold Approximation and Projection (UMAP) plot of the myeloid cell compartment isolated from public UUO scRNA-seq datasets, colored by unsupervised clustering. (B) Feature plots and violin plots displaying the expression of early pro-inflammatory "M1-like" markers (Tnf, Il1b, Cxcl10), predominantly enriched at day 3 post-UUO. (C) Feature plots and violin plots showing the expression of late pro-fibrotic "M2-like" markers (Mrc1Mrc1Mrc1, Arg1, Spp1), which dominate at days 7 and 14 post-UUO. (D) Monocle3 pseudotime trajectory analysis illustrating the continuous developmental transition of macrophages from an Il1b+ inflammatory state to an Spp1+ pro-fibrotic state over the course of fibrosis progression.

Published by Tehran University of Medical Sciences (http://ijaai.tums.ac.ir)

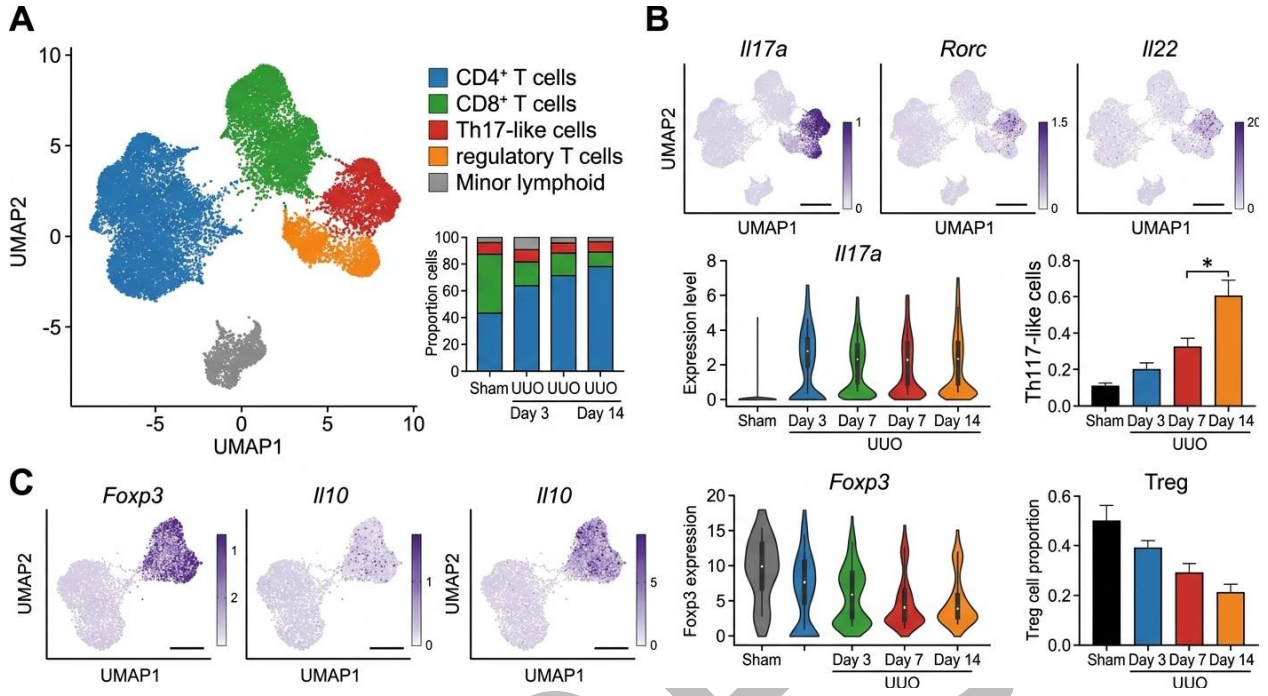

Figure 3. scRNA-seq reveals Th17 expansion and Treg depletion in the fibrotic kidney. (A) UMAP embedding of the re-clustered lymphoid compartment from the scRNA-seq datasets, highlighting distinct T-cell subpopulations. (B) Bar chart and feature plots demonstrating the significant expansion of the Th17-like cell cluster (marked by Il17a, Rorc, Il22) at day 14 post-UUO compared to sham and early time points ($p<0.01$). (C) Bar chart and feature plots showing the relative depletion of regulatory T-cells (Tregs, marked by Foxp3, Il10) over the same 14-day temporal window. Error bars represent standard deviation of cell proportions across biological replicates.

Table 2. T-cell subpopulation dynamics during fibrosis progression.

T-Cell Subset	Key Markers	Sham (%)	Day 3 (%)	Day 7 (%)	Day 14 (%)	*p* (Day 14 vs Sham)
Th1	**Ifng+, Tbx21+**	**25.4**	**38.2**	**31.5**	**22.1**	**0.15**
Th2	**Il4+, Gata3+**	**18.2**	**15.4**	**20.1**	**24.3**	**0.08**
Th17	**Il17a+, Rorc+**	**5.1**	**8.3**	**15.6**	**28.7**	**<0.001**
Treg	**Foxp3+, Il2ra+**	**15.3**	**12.1**	**8.4**	**4.2**	**<0.01**
CD8+ T-cell	**Cd8a+, Gzmb+**	**36.0**	**26.0**	**24.4**	**20.7**	**0.03**

Relative proportions (%) of identified T-cell subsets out of total lymphoid cells across sham, day 3, day 7, and day 14 UUO time points. Statistical significance (p-value) represents the comparison between Day 14 and Sham groups.

IN PRESS

CellChat Analysis Highlights Macrophage-T Cell-fibroblast Crosstalk

To understand the orchestration of the immune-fibrotic microenvironment, we inferred intercellular communication networks using *CellChat* (Figure 4A). The analysis revealed dense signaling interactions between Spp1+ macrophages, Th17 cells, and activated fibroblasts. We identified the Cxcl16-Cxcr6 ligand-receptor axis as a primary mechanism by which pro-fibrotic macrophages recruit T-cells to the injured kidney (Figure 4B). Furthermore, the communication probabilities indicated that Spp1+ macrophages are the dominant source of Tgfb1, sending strong paracrine signals to both Th17 cells (promoting their maintenance) and fibroblasts (driving ECM deposition), establishing a positive feedback loop of inflammation and fibrosis (Figure 4C).

Spatial Transcriptomics Confirms Co-localization of M2 Macrophages and Th17 Cells in Fibrotic Niches

To validate the predicted cellular interactions within the tissue architecture, we analyzed publicly available Visium spatial transcriptomics data from fibrotic murine kidneys (Figure 5A). By calculating and projecting the signature scores of the scRNA-seq derived clusters onto the spatial tissue coordinates, we observed highly restricted spatial patterning. The Spp1+ pro-fibrotic macrophage signature and the Il17a+ Th17 cell signature strongly co-localized within defined fibrotic niches (characterized by high Col1a1 and Acta2 expression) in the tubulointerstitium (Figure 5B). This spatial overlap confirms the CellChat predictions and demonstrates that these immune subsets physically interact within active zones of tissue remodeling (Figure 5C).

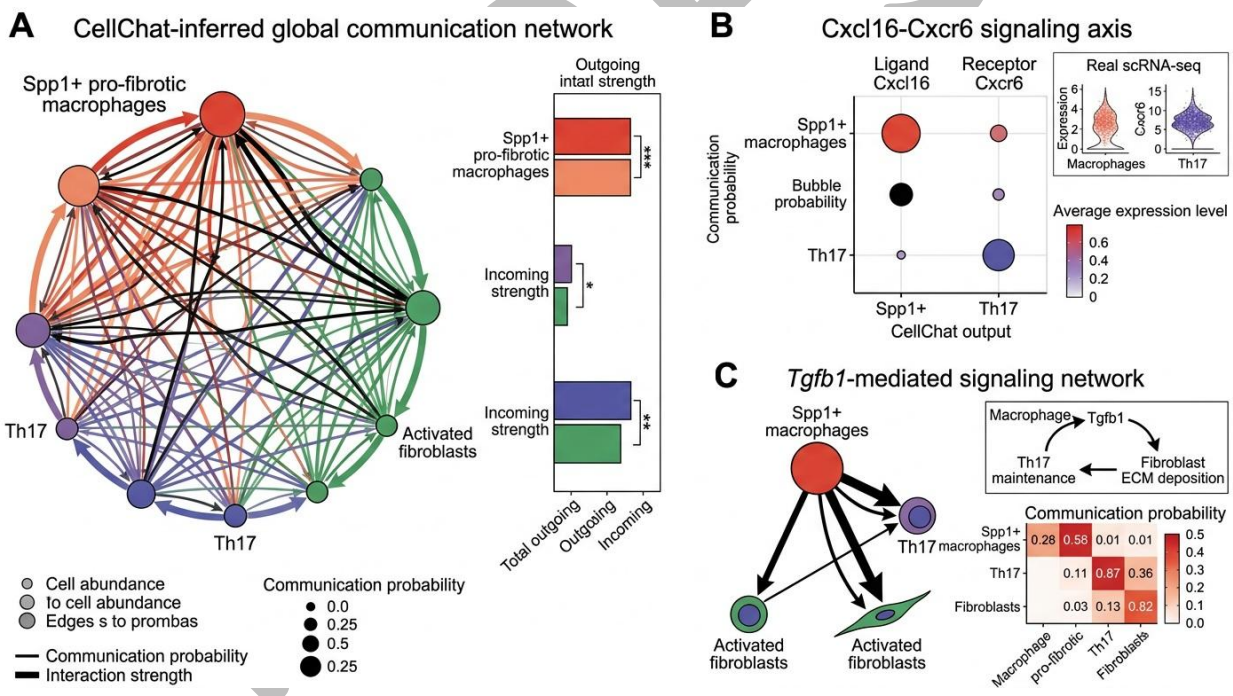

Figure 4. CellChat analysis infers complex macrophage-T cell-fibroblast communication networks.
(A) Circle plot summarizing the global number and strength of inferred intercellular communication networks among key scRNA-seq clusters. Edge width represents the probability of interaction. (B) Bubble plot detailing specific ligand-receptor interactions within the CXCL signaling pathway, highlighting the significant Cxcr6 axis responsible for T-cell recruitment by pro-fibrotic macrophages. (C) Network diagram of the TGF-β signaling pathway, illustrating Spp1+ macrophages as the primary sender of Tgfb1Tgfb1Tgfb1 signals to both Th17 cells (receivers) and activated fibroblasts (receivers), driving a pro-fibrotic feedback loop.

Published by Tehran University of Medical Sciences (http://ijaai.tums.ac.ir)

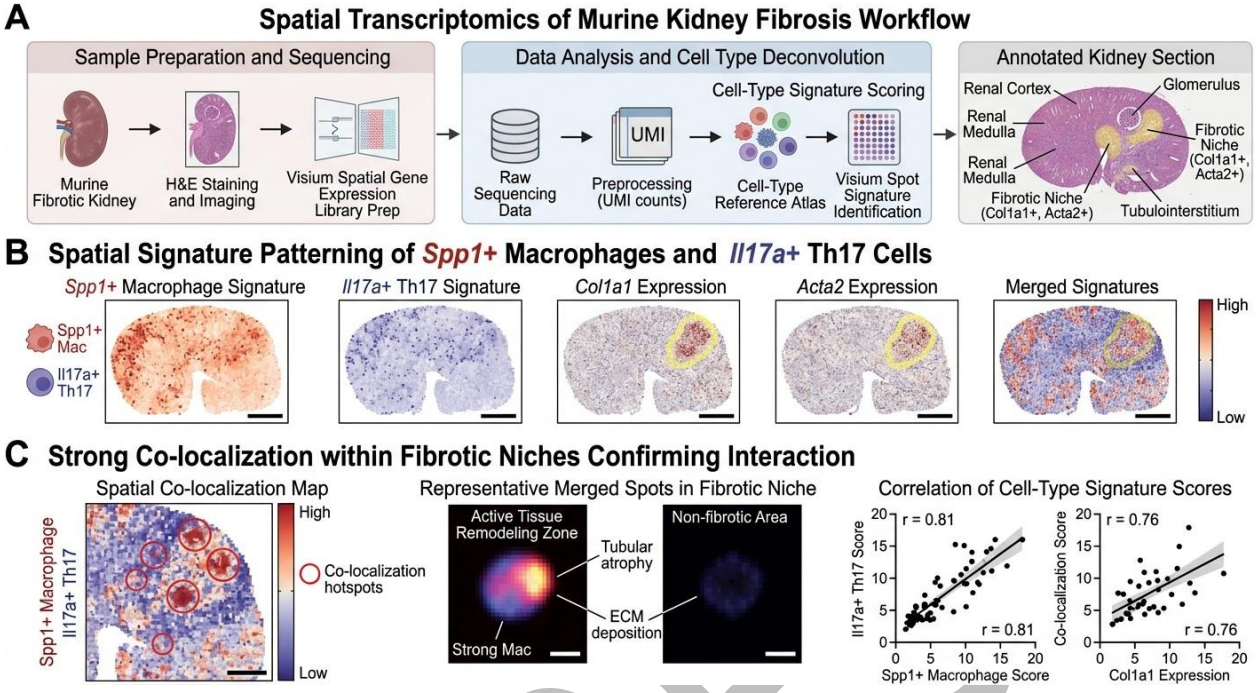

Figure 5. Spatial transcriptomics validates the co-localization of pro-fibrotic macrophages and Th17 cells in fibrotic niches. (A) Representative Hematoxylin and Eosin (H&E) reference image of a public Visium spatial transcriptomics slide from a day 14 UUO murine kidney. (B) Spatial feature plots projecting the module scores of the scRNA-seq derived Spp1+ macrophage signature and Il17a+ Th17 signature onto the tissue coordinates. Both signatures show highly restricted mapping to tubulointerstitial regions enriched for fibrotic markers (Col1a1, Acta2). (C) 2D density plot and spatial overlay confirming the high degree of spatial co-localization between Spp1+ macrophages and Th17 cells within the active zones of tissue remodeling.

DISCUSSION

In this study, we employed an integrative multi-omics approach to decipher the complex immunological landscape of renal fibrosis. Our integrated bioinformatics analysis revealed a dynamic, temporally regulated shift in macrophage polarization, a distinct imbalance in the Th17/Treg axis, and a critical communication network between macrophages and T-cells within the fibrotic niche.

Our scRNA-seq trajectory analysis demonstrated a clear phenotypic transition of macrophages from an early inflammatory state (high expression of Tnf and Il1b) to a late pro-fibrotic state (characterized by Mrc1 and Spp1 expression). This aligns with previous immunopathologic observations suggesting that persistent, unresolved inflammation seamlessly transitions into pathological tissue remodeling.[9] The identification of Spp1+ (Osteopontin) macrophages in the late stages of the UUO model is particularly noteworthy, as Osteopontin is a potent chemoattractant and a known driver of fibrosis.[10]

Furthermore, our analysis highlighted a significant disruption in the adaptive immune compartment, specifically an expansion of IL 17A+ Th17 cells and a concomitant depletion of Foxp3+ Tregs. Th17 cells are highly pro-inflammatory and have been implicated in autoimmune and allergic diseases; their accumulation in the fibrotic kidney may exacerbate ECM deposition through the sustained activation of fibroblasts.[11,12] The depletion of Tregs further removes the natural immunological brake on this process, perpetuating the cycle of injury and fibrosis.[13]

Crucially, our spatial transcriptomics and CellChat analyses bridged the gap between these distinct immune populations by identifying specific crosstalk mechanisms. The spatial co-localization of M2-like macrophages and Th17 cells suggests a localized "fibrotic niche" where intense intercellular signaling occurs. The prominent CXCL16-CXCR6 signaling axis identified in our study provides a mechanistic explanation for the continuous recruitment of pathogenic T-cells to these specific anatomical zones [14].

IN PRESS

Interrupting this chemokine axis or targeting the downstream TGF-β signaling pathways identified in our macrophage-fibroblast interaction networks may offer novel immunotherapeutic strategies for CKD.[15] Biologically, the CXCL16-CXCR6 axis is critical for mediating the recruitment and retention of pro-inflammatory macrophages and T-cells to the injured renal interstitium, thereby sustaining the inflammatory niche. Subsequently, the enriched TGF-β signaling acts as a master profibrotic regulator within these cellular interaction networks, driving the activation of resident fibroblasts into myofibroblasts and accelerating excessive extracellular matrix deposition.

This study has several limitations. First, as a purely bioinformatics-driven investigation utilizing public datasets, the findings are constrained by the original experimental designs and sequencing depths of the source studies. Second, while the integration of scRNA-seq and spatial transcriptomics provides robust predictive models, these immunological interactions require extensive *in vitro* and *in vivo* experimental validation. Future studies should focus on functional assays to block the identified receptor-ligand pairs (e.g., the CXCR6 axis) to confirm their therapeutic potential.

In conclusion, our multi-omics profiling maps the intricate immune-fibrotic axis in renal fibrosis, highlighting the temporal dynamics of macrophage plasticity and Th17 cell infiltration. These insights provide a foundational immunological framework for developing targeted immunotherapies aimed at halting or reversing chronic kidney disease.

STATEMENT OF ETHICS

This study was conducted in accordance with the Declaration of Helsinki (2013). The study protocol was approved by the Institutional Review Board (IRB) of Shahid Beheshti University of Medical Sciences (Reference code: IR.SBMU.MSP.REC.1403.257).

FUNDING

The authors declare that no funds, grants, or other support were received during the preparation of this manuscript

CONFLICT OF INTEREST

The authors declare no conflicts of interest.

ACKNOWLEDGMENTS

Not applicable.

DATA AVAILABILITY

The datasets analyzed during the current study are available in the NCBI Gene Expression Omnibus (GEO) public repository. Single-cell RNA-sequencing and spatial transcriptomics data were accessed under the accession numbers GSE131685, GSE114156, and GSE173343. Bulk transcriptomic data were retrieved under the accession number GSE150338. The supplementary machine learning and data processing R codes generated during this study are included in the supplementary material. Further detailed code and processed data matrices are available from the corresponding author upon reasonable request.

AI ASSISTANCE DISCLOSURE

The authors reviewed and edited all AI-generated suggestions and take full responsibility for the content of this manuscript. No AI tool was used to generate data, analyses, figures, or references.

REFERENCES

1. Kalantar-Zadeh K, Jafar TH, Nitsch D, Neuen BL, Perkovic V. Chronic kidney disease. Lancet. 2021;398(10302):786-802.
2. Humphreys BD. Mechanisms of renal fibrosis. Annu Rev Physiol. 2018;80:309-26.
3. Kurts C, Panzer U, Anders HJ, Rees AJ. The immune system and kidney disease: basic concepts and clinical implications. Nat Rev Immunol. 2013;13(10):738-53.
4. Sato Y, Yanagita M. Immune cells and inflammation in AKI to CKD progression. Am J Physiol Renal Physiol. 2018;315(6):F1501-12.
5. Tang PM, Nikolic-Paterson DJ, Lan HY. Macrophages: versatile players in renal inflammation and fibrosis. Nat Rev Nephrol. 2019;15(3):144-58.
6. Meng XM, Nikolic-Paterson DJ, Lan HY. TGF-β: the master regulator of fibrosis. Nat Rev Nephrol. 2016;12(6):325-38.
7. Chung SA, Farris AB 3rd, Uehara H, et al. Imbalance of Th17 and Treg cells in the pathogenesis of chronic kidney disease. Kidney Int. 2020;98(3):711-23.

IN PRESS

8. Wu H, Uchimura K, Donnelly EL, Kirita Y, Morris SA, Humphreys BD. Comparative analysis and refinement of human PSC-derived kidney organoid differentiation with single-cell transcriptomics. Cell Stem Cell. 2018;23(6):869-81.
9. Huen SC, Cantley LG. Macrophages in renal injury and repair. Annu Rev Physiol. 2017;79:449-69.
10. Riwaldt S, Coryell PR, Revelo XS. Spp1+ macrophages in tissue repair and fibrogenesis. Front Immunol. 2022;13:958432.
11. Paust HJ, Turner JE, Steinmetz OM, et al. The IL-23/Th17 axis contributes to renal injury in experimental glomerulonephritis. J Am Soc Nephrol. 2009;20(5):969-79.
12. Ramani K, Biswas PS. Interleukin-17: A crucial cytokine in tissue pathology and immune regulation in kidney diseases. Eur J Immunol. 2019;49(3):364-74.
13. Sharma A, Rudra D. Emerging functions of regulatory T cells in tissue homeostasis. Front Immunol. 2018;9:883.
14. Xia Y, Entman ML, Wang Y. Critical role of CXCL16 in hypertensive kidney injury and fibrosis. Hypertension. 2013;62(6):1129-37.
15. Lv W, Booz GW, Wang Y, Fan F, Roman RJ. Macrophage-mediated inflammatory networks and therapeutic interventions in chronic kidney disease. Pharmacol Rev. 2024;76(1):15-42.

IN PRESS